TELKOMNIKA Telecommunication, Computing, Electronics and Control
Vol. 18, No. 4, October 2020, pp. 2718~2728
ISSN: 1693-6930, accredited First Grade by Kemenristekdikti, Decree No: 21/E/KPT/2018
DOI: 10.12928/TELKOMNIKA.v18i5.14377

Modeling and control of double star induction machine by active disturbance rejection control

Aichetoune Oumar[1], Rachid Chakib[2], Mohamed Cherkaoui[3]
[1,3]Mohammedia School of Engineers, Mohammed V University, Morocco
[2]Laboratory of Innovation in Management and Engineering for Enterprise, Morocco

Article Info

Article history:

Received Oct 20, 2019
Revised Apr 7, 2020
Accepted May 1, 2020

Keywords:

ADRC
DSIM
ESO
MLI

ABSTRACT

This paper aims to contribute to the modeling and control of the double star induction machine (DSIM) by a robust method called active disturbance rejection control (ADRC). The ADRC has become in the last decade one of the most important techniques of regulation. This method is based on the use of an ESO (Extended State Observer) which estimates in real-time and at the same time the external disturbances and the errors due to the variations of the parameters of the machine and to the uncertainties of modeling. The two stators of DSIM are powered by three-phase inverters based on transistors and MLI control and the entire system is modeled in Park's reference. We analyze in the Matlab/Simulink environment the dynamic behavior of the system and the different ADRC controllers under different operating conditions. The result has demonstrated the performance and effectiveness of the ADRC.

Corresponding Author:

Aichetoune Oumar,
Department of Electrical Engineering, Mohammedia School of Engineers,
University V Mohammed,
Rabat, Morocco.
Email: aichetouna.mahmoud@gmail.com

1. INTRODUCTION

The increase of the power of the electrical machines brings to light several problems as well at the level of the machine as of the inverter which provides its power. The static switches of the inverter must be sized to switch large currents which result in more power loss and accelerated aging of the electronic components of the inverter. The poly-phase machines offer a very interesting alternative to reducing stress on machine windings and converter switches [1].

These machines are usually composed of several stators allowing segmentation and reduction of power per phase. The use of the double star induction machine (DSIM) has increased considerably in recent years [2], especially in high-power applications such as rail traction, ship propulsion, electrical and hybrid vehicles, among others [2, 3]. The configuration of the DSIM is similar to a three-phase asynchronous cage machine with two stator windings offset in space by an angle generally equal to $\pi/6$. Each star winding is powered by a power electronics converter [4].

The double star induction machine has several advantages over the three-phase asynchronous machine such as the distribution of power over several phases, the possibility of torque reduction and improved reliability thanks to the ability to operate the DSIM with one or more phases in default [5, 6]. However, the DSIM still has some problems mainly related to the rate of harmonics in currents due to the presence of power converters, the non-linearity of its dynamic model and the complexity of its control [7].

The mathematical model of DSIM in the three-phase reference and Park's reference is similar to that of the three-phase induction machine, but with a higher number of magnitudes and equations. In this article we have chosen to use vector control with field-oriented control to operate the DSIM as an independent excitation DC machine, allowing for decoupling between electromagnetic torque and rotor flux [8]. The purpose of this decoupling is to control the speed of the machine and to maintain constant rotor flux.

The control of the double star induction machine is often by a PI regulator. This regulator has shown in reference [7] their performances and effectiveness in the control of DSIM. But it has some difficulty in parameter variations and load disturbance. The problem posed by the sensitivity lead the PI regulator to lose its performance. In this context, researchers are seeking to replace it with other regulation techniques to avoid sensitivity to the variation of machine parameters. Due to the limitation presented by the PI regulator and to improve the control of DSIM, we use a robust control strategy based on the control of DSIM rotor currents by ADRC (active disturbance rejection control) control loops.

The ADRC is a non-linear regulator that estimates and compensates in real-time the external disturbances and internal disturbances due to modeling uncertainties and machine parameter variations [9, 10]. This ADRC control strategy is based on an extended state observer known as ESO (Extended State Observer), which allows instantaneous estimation of all disturbances affecting the machine [9, 10]. This estimation is used in the generation of the control signal allowing the decoupling of the system from its disturbances [10].

The outline of this paper is organized as follows. Section 2 is devoted to the modeling of DSIM. We develop also the principle and performance of the ADRC control strategy, then its implementation for the vector control of DSIM. In section 3, we present the results of the study of the dynamic behavior of the machine under different operating conditions. And a conclusion is taken in section 4.

2. RESEARCH METHOD

2.1. DSIM model

2.1.1. Representation of the DSIM

The DSIM studied in this article is squirrel- cage induction motor. Its stator is composed of two coils coupled in star and offset by an angle $\alpha = \pi/6$ [11]. Figure 1 illustrates the rotor and stator windings of the DSIM [12]. With θ_1, θ_2 are respectively the angles between the rotor phase ra and the stator phases (sa_1) and (sa_2). α is the offset angle between the star windings (sa_1) and (sa_2).

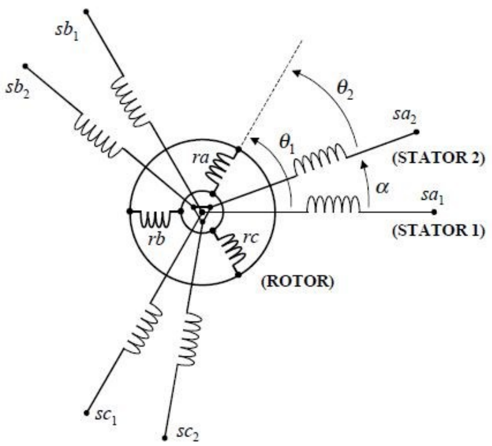

Figure 1. DSIM windings

2.1.2. Park reference of DSIM model

Park's model consists of transforming a three-phase system (A, B, C) into a two-phase system (d, q), while maintaining power and the electromotive force. Figure 2 shows the rotor and stator windings of the DSIM in the Park reference [13]. Where θs_1, θs_2, θ_r are respectively the angles between the axis d and the stator phases (sa_1), (sa_2) and the rotor phase ra.

The equations of the voltages, in the two-phase reference (d, q) are expressed by the system of (1) [12-14]:

$$\begin{cases} V_{ds1} = R_{s1} i_{ds1} + \frac{d\psi_{ds1}}{dt} - \omega_s \psi_{qs1} \\ V_{ds2} = R_{s2} i_{xs2} + \frac{d\psi_{ds2}}{dt} - \omega_s \psi_{qs2} \\ V_{qs1} = R_{s1} i_{qs1} + \frac{d\psi_{qs1}}{dt} + \omega_s \psi_{ds1} \\ V_{qs2} = R_{s2} i_{qs2} + \frac{d\psi_{qs2}}{dt} + \omega_s \psi_{ds2} \\ 0 = R_r i_{dr} + \frac{d\psi_{dr}}{dt} - \omega_{gl} \psi_{qr} \\ 0 = R_r i_{qr} + \frac{d\psi_{qr}}{dt} + \omega_{gl} \psi_{dr} \end{cases} \tag{1}$$

with $\omega_{gl} = \omega_s - \omega_r$.
The flux [12-14]:

$$\begin{cases} \psi_{ds1} = L_{s1} i_{ds1} + L_m(i_{ds1} + i_{ds2} + i_{dr}) \\ \psi_{ds2} = L_{s2} i_{ds2} + L_m(i_{ds1} + i_{ds2} + i_{dr}) \\ \psi_{qs1} = L_{s1} i_{qs1} + L_m(i_{qs1} + i_{qs2} + i_{qr}) \\ \psi_{qs2} = L_{s1} i_{qs2} + L_m(i_{qs1} + i_{qs2} + i_{qr}) \\ \psi_{dr} = L_r i_{dr} + L_m(i_{ds1} + i_{ds2} + i_{dr}) \\ \psi_{qr} = L_r i_{qr} + L_m(i_{qs1} + i_{qs2} + i_{qr}) \end{cases} \tag{2}$$

The expression of torque [14, 15]:

$$C_e = P \frac{L_m}{L_m + L_r} (\psi_{dr}(i_{qs1} + i_{qs2}) - \psi_{qr}(i_{ds1} + i_{ds2})) \tag{3}$$

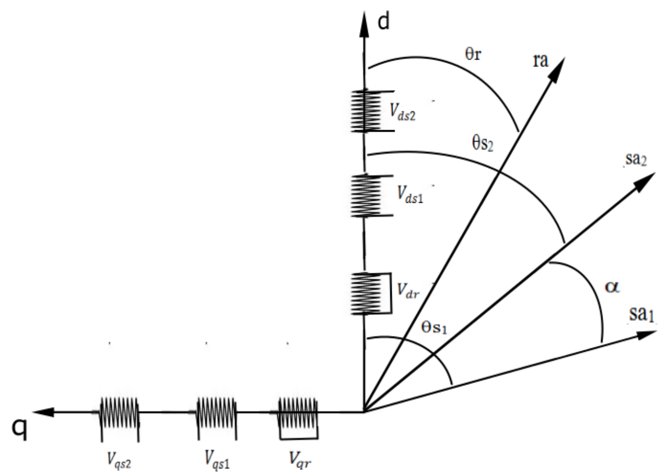

Figure 2. DSIM model in Park's reference

2.2. Active disturbance rejection control strategy

The active disturbance rejection control was introduced by Han in 1995 [16]. It is a robust command based on the extension of the system model by a supplemental and fictitious state variable representing all the user cannot control in the mathematical model of the system controlled [17]. All real disturbances and modeling uncertainties are represented in this virtual state, the estimation of which is ensured by an extended state observer (ESO) [18-21]. Using this estimated state, a control signal is generated to decouple the system from the actual disturbance acting process. The ADRC application allows the user to treat the system as a simpler model because the negative effects of external disturbances and uncertainties of modeling are compensated in real time.

To illustrate the principle of the ADRC, we consider the following system first order [22, 23]:

$$y'(t) = f(t) + b_0 U(t) \tag{4}$$

with, $U(t)$ and $y(t)$ are the input and output magnitudes of the system. $f(t)$ represents the sum of external disturbances, modeling errors and / or changes in system parameters. b_0 is a parameter known from the system under study. The state variable representation of the first-order system is described as follows [24]:

$$\begin{cases} \dot{x}_1 = x_2 + b_0 U \\ \dot{x}_2 = \dot{f} \\ y = x_1 \end{cases} \tag{5}$$

The basic idea of the ADRC is to implement an extended state observer (ESO) that provides an estimate $\hat{f}(t)$ such that the effect of $f(t)$ on the system can be compensated. The system control scheme is illustrated by the Figure 3 [25, 26]:

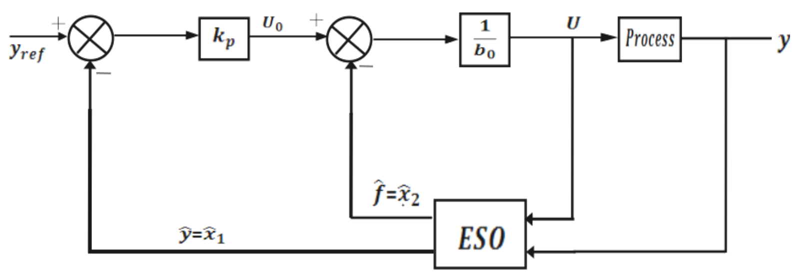

Figure 3. ADRC structure of a first order system

k_p is the gain of the proportional regulator which acts on $\hat{y}(t)$rather than on the actual output $y(t)$. Its value is chosen according to the desired response time of the system studied in a closed loop. ESO is a Luenberger's observer that estimates the internal state variables of the system from the control input and the output.

The structure of this observer is expressed by the following model [24-27]:

$$\begin{cases} \dot{\hat{x}}(t) = (A - LC)\hat{x}(t) + Bu(t) + Ly(t) \\ \hat{y}(t) = C\hat{x}(t) \end{cases} \tag{6}$$

with $A - LC = \begin{pmatrix} -\beta_1 & 1 \\ -\beta_2 & 0 \end{pmatrix}$; $B = \begin{pmatrix} b_0 \\ 0 \end{pmatrix}$; $L = \begin{pmatrix} \beta_1 \\ \beta_2 \end{pmatrix}$; $C = (1 \;\; 0)$

β_1 , β_2 are the gains of the extended state observer and are generally determined by the pole placement technique. The rigorous determination of these gains makes it possible to guarantee to the observer a speed and sensitivity to the appropriate noises.

$$\beta_1 = 2 * \omega_0 \,, \beta_2 = {\omega_0}^2$$

ω_0 and ω_c are respectively the ESO cut-off (break) pulse and the closed loop system cut-off pulse. The poles of the observer should be placed to the left of the pole of the closed loop to have faster dynamics.

$$\omega_0 = 3{\sim}10\omega_c, \qquad \omega_c = k_p$$

2.3. Implementation of ADRC in DSIM control

2.3.1. Vector control

To make the control of the electromagnetic torque of the DSIM independent from the rotor flux, we orient the latter in the direct axis of Park's reference and we keep it constant [28]:

$$\begin{cases} \psi_{dr} = \psi_r \\ \psi_{qr} = 0 \end{cases} \tag{7}$$

The electromagnetic torque is thus expressed by:

$$C_e = P \frac{L_m}{L_m + L_r} \left(\psi_r \left(i_{qs1} + i_{qs2} \right) \right) \tag{8}$$

The flux expressions of (2) become:

$$\begin{cases} \psi_{ds1} = (L_{s1}+e)i_{ds1} + e i_{ds2} + d\,\psi_r \\ \psi_{ds2} = e i_{ds1} + (L_{s1}+e)i_{ds2} + d\,\psi_r \\ \psi_{qs1} = (L_{s1}+e)i_{qs1} + e i_{qs2} \\ \psi_{qs2} = e i_{qs1} + (L_{s1}+e)i_{qs2} \\ i_{dr} = \frac{\psi_r - L_m(i_{ds1}+i_{ds2})}{L_r+L_m} \\ i_{qr} = \frac{-L_m(i_{qs1}+i_{qs2})}{L_r+L_m} \end{cases} \quad (9)$$

with e and d are constants:

$e = \frac{L_m L_r}{L_r+L_m}$, $d = \frac{L_m}{L_r+L_m}$.

By replacing in (1), the expressions of rotor flux and currents given by (9), we express the direct and quadrature components of the stator voltages by:

$$V_{ds1} = R_{s1}i_{ds1} + L_{s1}\frac{di_{ds1}}{dt} - \omega_s((L_{s1}+e)i_{qs1} + e i_{qs2}) \quad (10)$$

$$V_{qs1} = R_{s1}i_{qs1} + L_{s1}\frac{di_{qs1}}{dt} + \omega_s((L_{s1}+e)i_{ds1} + e i_{ds2} + d\psi_r) \quad (11)$$

$$V_{ds2} = R_{s2}i_{ds2} + L_{s2}\frac{di_{ds2}}{dt} - \omega_s(e i_{qs1} + (L_{s2}+e)i_{qs2}) \quad (12)$$

$$V_{qs2} = R_{s1}i_{qs2} + L_{s2}\frac{di_{qs2}}{dt} + \omega_s(e i_{ds1} + (L_{s2}+e)i_{ds2} + d\psi_r) \quad (13)$$

for a decoupling between the quantities d and q, we put these expressions of tension in the form:

$$V_{ds1} = V_{d1} + e_{ds1} \quad (14)$$

$$V_{qs1} = V_{q1} + e_{qs1} \quad (15)$$

$$V_{ds2} = V_{d2} + e_{ds2} \quad (16)$$

$$V_{qs2} = V_{q2} + e_{qs2} \quad (17)$$

with:

$$e_{ds1} = -\omega_s((L_{s1}+e)i_{qs1} + e i_{qs2}) \quad (18)$$

$$e_{qs1} = \omega_s((L_{s1}+e)i_{ds1} + e i_{ds2} + d\psi_r) \quad (19)$$

$$e_{ds2} = -\omega_s(e i_{qs1} + (L_{s2}+e)i_{qs2}) \quad (20)$$

$$e_{qs2} = \omega_s(e i_{ds1} + (L_{s2}+e)i_{ds2} + d\psi_r) \quad (21)$$

and

$$V_{d1} = R_{s1}i_{ds1} + L_{s1}\frac{di_{ds1}}{dt} \quad (22)$$

$$V_{q1} = R_{s1}i_{qs1} + L_{s1}\frac{di_{qs1}}{dt} \quad (23)$$

$$V_{d2} = R_{s2}i_{ds2} + L_{s2}\frac{di_{ds2}}{dt} \quad (24)$$

$$V_{q2} = R_{s1} i_{qs2} + L_{s2} \frac{di_{qs2}}{dt} \tag{25}$$

Figure 4 shows the direct field-oriented control (DFOC) used for the control of the DSIM. This method is based on the estimation of the rotor flux module (ψ_r) and the phase(θ_s).

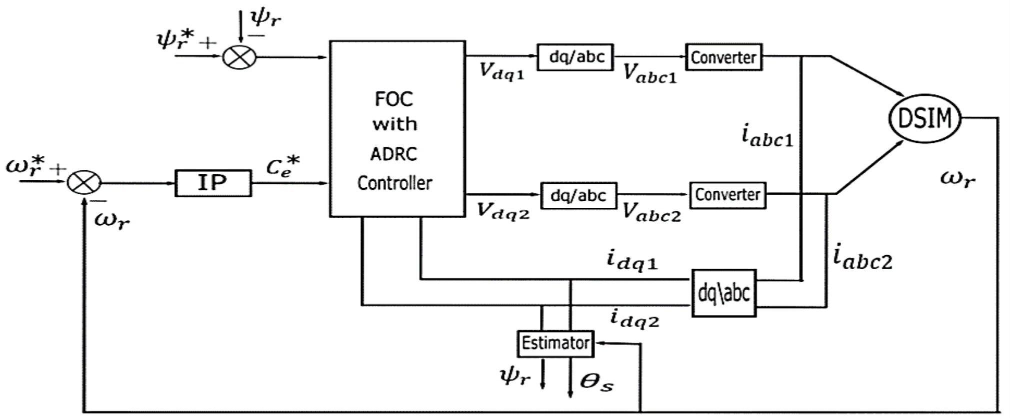

Figure 4. Direct field-oriented control of the DSIM

– Estimation of ψ_r

From the systems of (1) and (2) we deduce:

$$\frac{d\psi_r}{dt} = \frac{R_r L_m}{L_r + L_m}(i_{ds1} + i_{ds2}) - \frac{R_r}{L_r + L_m}\psi_r \tag{26}$$

hence the expressions of the rotor flux:

$$\psi_r = \frac{L_m}{1 + Tr.s}(i_{ds1} + i_{ds2}) \tag{27}$$

with $Tr = \frac{L_r + L_m}{R_r}$

– Estimation de θ_s

$$\theta_s = \int \omega_s dt \tag{28}$$

where $\omega_s = \omega_{gl} + \omega_r$

The expression of ω_{gl} is obtained from (1) and (2):

$$\omega_{gl} = \frac{R_r L_m}{L_r + L_m} \frac{(i_{qs1} + i_{qs2})}{\psi_r} \tag{29}$$

$$\theta_s = \int (\omega_r + \frac{R_r L_m}{L_r + L_m} \frac{(i_{qs1} + i_{qs2})}{\psi_r})\, dt \tag{30}$$

2.3.2. Synthesis of the ADRC regulators

The strategy consists of controlling the stator currents of the DSIM by ADRC regulators. From (22-25), the stator currents of the DSIM can be expressed by:

$$\frac{di_{ds1,2}}{dt} = -\frac{R_{s1}}{L_s} i_{ds1,2} + \frac{1}{L_s} V_{d1,2} \tag{31}$$

and

$$\frac{di_{qs1,2}}{dt} = -\frac{R_{s1}}{L_s} i_{qs1,2} + \frac{1}{L_s} V_{q1,2} \tag{32}$$

We put these expressions in the following form:

$$\frac{di_{ds1,2}}{dt} = f_{d1,2}(t) + b_{0d1,2}U_{d1,2}(t) \tag{33}$$

and

$$\frac{di_{qs1,2}}{dt} = f_{q1,2}(t) + b_{0q1,2}U_{q1,2}(t) \tag{34}$$

with: $f_{d1,2}(t) = -\frac{R_s}{L_s}i_{ds1,2} + (\frac{1}{L_s} - b_{0d1,2})V_{d1,2};\ U_{d1,2}(t) = V_{d1,2}; b_{0d1,2} = \frac{1}{L_s}$

and: $f_{q1,2}(t) = -\frac{R_s}{L_s}i_{qs1,2} + (\frac{1}{L_s} - b_{0q1,2})V_{q1,2}; U_{q1,2}(t) = V_{q1,2}; b_{0q1,2} = \frac{1}{L_s}$

$f_{d1,2}(t)$ and$f_{q1,2}(t)$ represent the total disturbances respectively affecting the currents *isd₁*, *isd₂*, *isq₁ and isq₂*. $U_{d1,2}(t)$and$U_{q1,2}(t)$are respectively the control inputs of the current control loops isd_1, isd_2, $isq_1$and isq_2. $b_{0d1,2}$ and $b_{0q1,2}$ are the known parts of the system parameters. By choosing a suitable response time, we easily determine the parametersk_p, β_1 and β_2 of the ADRC regulators so that the stator currents follow perfectly their references as shown in Figure 5.

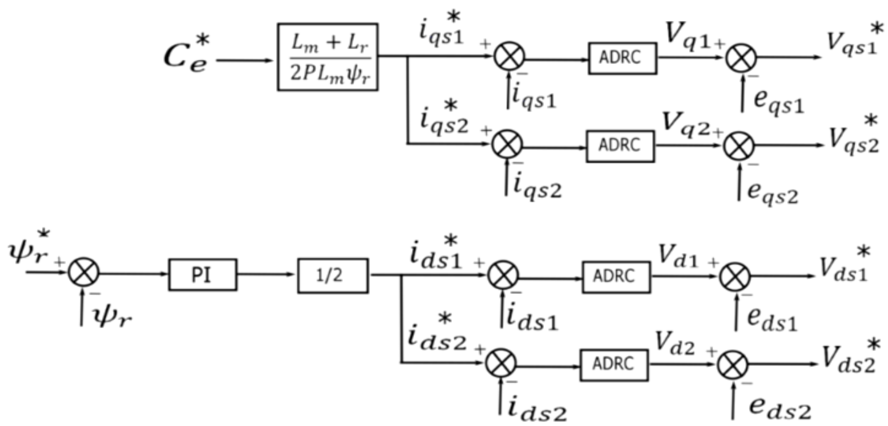

Figure 5. Direct method (DFOC)

3. RESULTS AND ANALYSIS

In order to verify the performance and the robustness of the active disturbance rejection control applied to the DSIM, the machine model and its vector control using the ADRC regulators are simulated in the Matlab/Simulink environment. The DSIM studied in this paper is fed by two voltage inverters at two levels, its electrical and mechanical parameters with the regulators gain are given in the appendix. In this section, three tests are simulated. The first test is devoted to illustrating the response of the machine in the load variation test. In the second test, we invert the speed direction. The third test is the robustness test.

3.1. Load variation test

The DSIM runs empty until time t = 2 s, when we introduce a load torque of 16 N.m, at t = 4 s we change the load torque from 16 N.m to 10 N.m. We note from Figure 6 that the speed of the DSIM follows its reference even after the load variation from 0 to 16 and from 16 to 10. Almost no overtaking or disturbance can move the speed away from its reference.

We also find that the electromagnetic torque varies proportionally to the stator currents in quadrature isq1 and isq2, and it is independent of the rotor flux which is kept constant. The currents of each stator winding of the DSIM are perfectly sinusoidal and their amplitudes depend on the load conditions. The control strategy implemented based on ADRC regulators perfectly achieves a decoupling between the electromagnetic torque of the DSIM and the rotor flux.

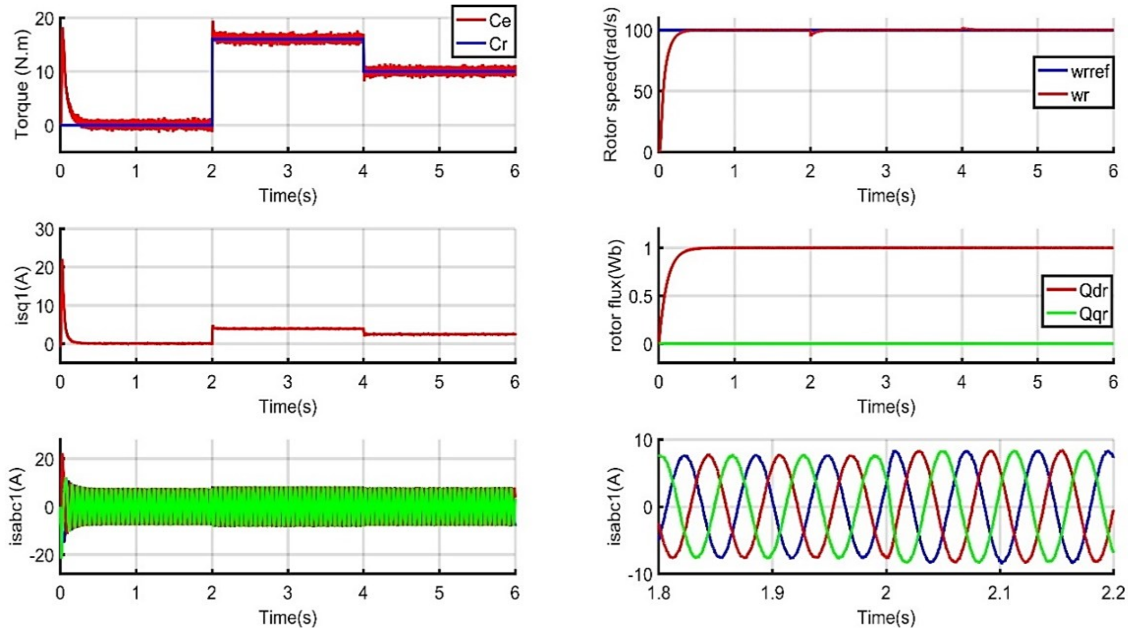

Figure 6. Operation of the DSIM controlled by ADRC regulators with load variation

3.2. Speed inversion test

This test consists to simulate the ADRC command with changing speed reference at 4s and by applying a load of 16 N.m at t = 2 s. Figure 7 illustrates the evolution of electrical quantities and mechanics of the DSIM under these operating conditions. The rotation speed ω_r changes direction at t = 4 s and goes from 100 rad/s to -100 rad/s after a transient regime about 0.35 s.

This inversion of speed direction is accompanied by a change in the order of the phases of the stator currents, a disturbance of the electromagnetic torque and the current isq1 for a short time before they return to their initial reference values. The rotor flux is maintained constant and independent of the variation of the torque. The estimation and the compensation of the external disturbances, due to the variation of the load and the change of reference speed, by the ADRC regulators allowed the system to have very satisfactory performance.

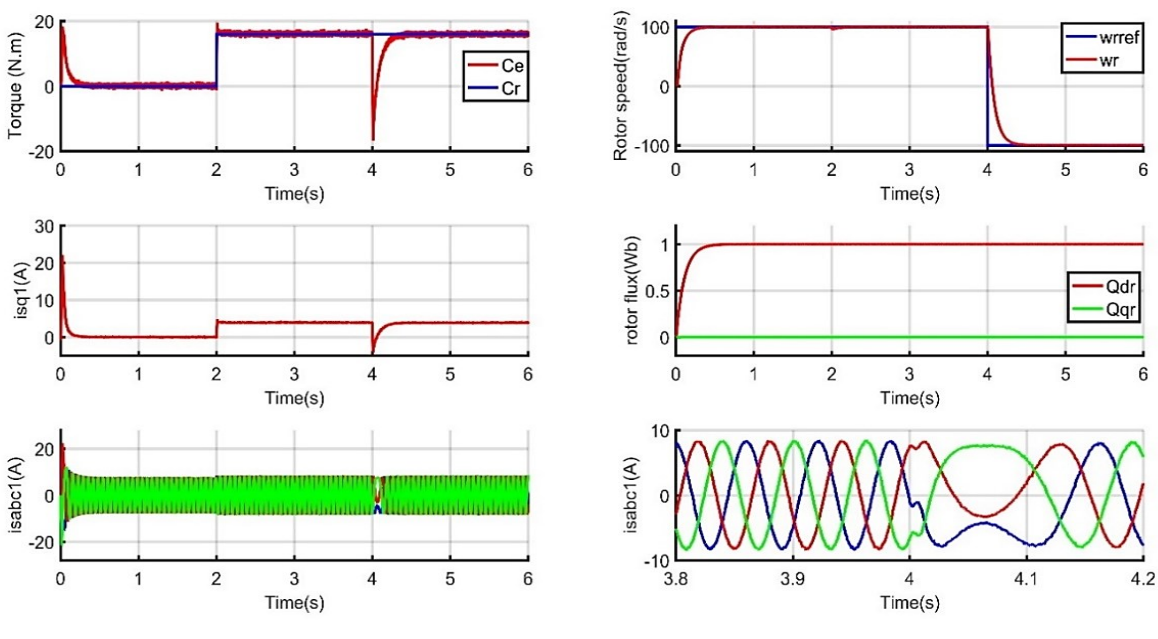

Figure 7. Operation of the DSIM with inversion speed

3.3. Robustness test

The robustness test consists of varying the rotor resistor R_r, the moment of inertia J and the stator inductances of the DSIM. Indeed, the regulators' calculations are based on functions whose parameters are assumed to be fixed. However, in a real system, these parameters are subject to variations driven by different physical phenomena.

Figure 8 shows the evolution of the stator currents, the speed of rotation and the electromagnetic torque of the DSIM during a variation of 100% of the value of the rotor resistance R_r, the moment of inertia J and the stator inductances at time of 3 s. The variations of these parameters have almost no influence on the machine's operation because the ADRC controllers make it possible to automatically compensate for the disturbances due to these variations. The tracking of the reference is still ensured and the stability of the system is not affected by these parameter variations.

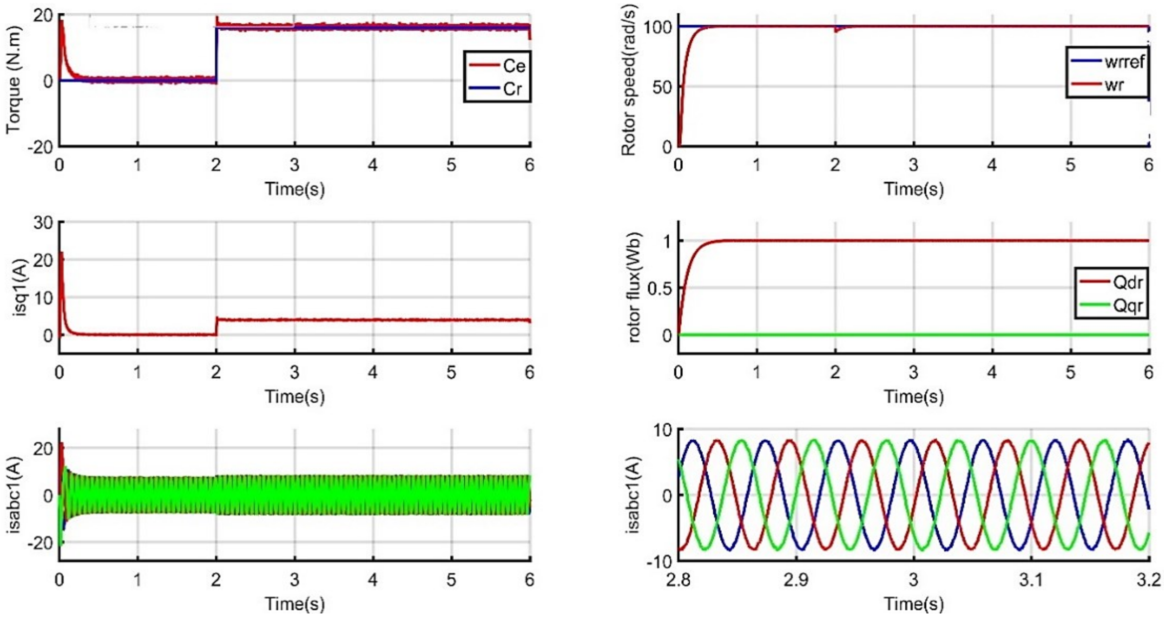

Figure 8. Operation of the DSIM with rotor resistor variation, the moment of inertia variation and the stator inductances variations ($R_r = 2*R_{rn}$, $J= 2*J_n$ and $L_{s1,2} =2* L_{s1,2}$) at t=3s

4. CONCLUSION

This paper is dedicated to present control of DSIM using the ADRC command. The model of the double star induction machine in the Park reference system has been developed and the ADRC theories are also presented. This command allows the compensation of all external disturbances, modeling errors and parametric variations of the system. These disturbances represent the main concern in electrical drive systems. We have seen through the results obtained in this article, that the control by the active disturbance rejection control ADRC offers very good performances and robustness because it allows having a stable operation by eliminating the effect of the disturbances due mainly to the variation of the machine parameters, the variation of the load conditions and the change of the speed of rotation. The control by ADRC can be a very interesting solution for the systems using double star induction machine such as electrical vehicles, rail traction, marine electric propulsion and wind generators to name but few.

APPENDIX

Parameters of the DSIM:
Rated power 4.5 KW
Number of pole pairs $P = 2$
Stator and rotor resistors:
$R_{S1}= R_{S2} =0.86\Omega$, $R_r =0.36\Omega$.
Stator and rotor inductances:
$L_{S1}= L_{S2} =0.184H$, $L_r =0.0246H$.

Mutual inductance: L_m =*0.0537H*
Moment of inertia: *J = 0.025 kg.m2*
Coefficient of friction: K_f = *0.001Nms/rad*
Parameters of the ADRC regulators of the stator currents: $K_P = 379.1709$, *b0 = 5.4348,* β_1= *7.5834e+03,* β_2=*1.4377e+07.*
Parameters of the PI regulators of the rotor flux: $K_{P\psi_r} = 37.7358, K_{i\psi_r} = 175.0632$.
Parameters of the PI regulators of speed: $K_{P\omega_r} = 1.1865, K_{i\omega_r} = 11.8850$.

REFERENCES

[1] Akpama E. J., Anih L. U., "Modelling and Simulation of Multiphase Induction Machine," *International Journal of Engineering Innovation &Research,* vol. 4, no. 5, pp. 732-736, 2015.

[2] Slimene M. B., Khlifi M. A., "Modeling and digital field-oriented control for double star induction motor drive," *International Journal of Applied Electromagnetics and Mechanics*, vol. 56, no. 4, pp. 511-520, 2018.

[3] Azib A., Ziane D., Rekioua T., Tounzi A., "Robustness of the direct torque control of double star induction motor in fault condition," *Rev. Roum. Sci. Tech. Élect. et Énerg,* vol. 61, no. 2, pp. 147-152, 2016.

[4] Tir Z., Soufi Y., Hashemnia M. N., Malik O., Marouani K., "Fuzzy logic field oriented control of double star induction motor drive," *Electrical Engineering,* vol. 99, pp. 495-503, 2017.

[5] Layadi N., Djerioui A., Zeghlache S., Mekki H., Houari A., Benkhoris M., Berrabah F., "New Fault Tolerant Control Based on Backstepping Controller for Double Star Induction Machine," *Rev. Roum. Sci. Techn.-Électrotechn. et Énerg.,* vol. 64, no. 3, pp. 275-280, 2019.

[6] Boukhalfa G., Belkacem S., Chikhi A., Benaggoune S., "Direct torque control of dual star induction motor using a fuzzy-PSO hybrid approach," *Applied Computing and Informatics*, pp. 1-17, 2018.

[7] Merabet E., Abdessemed R., Amimeur H., Hamoudi F., "Field Oriented Control of a Dual Star Induction Machine Using Fuzzy Regulators, *CIP. Sétif*, pp. 1-7, 2007.

[8] Lazreg M. H., Bentaallah A., "Speed sensorless vector control of double star induction machine using reduced order observer and MRAS estimator," *The 5th International Conference on Electrical Engineering Boumerdes (ICEE-B),* pp. 1-6, 2017.

[9] Wang F., Liu E., Wang R., Zhang W., Yang Y., "An approach to improve active disturbance rejection control," *International Journal of Control*, vol. 93, no. 5, pp. 1063-73, 2020.

[10] Chalawane H., Essadki A., Nasser T., Arbaoui M., "A New Robust Control Based on Active Disturbance Rejection Controller for Speed Sensorless Induction Motor," *3rd International Conference on Electrical and Information Technologies (ICEIT),* pp. 1-6, 2017.

[11] Abden A., Bouchetta A., Boughazi O., Baghdadi A., Bousserhane I. K., "Double star induction machine using nonlinear integral backstepping control," *International Journal of Power Electronics and Drive System,* vol. 10, no. 1, pp. 27-40, 2019.

[12] Youb L., Belkacem S., Naceri F., Cernat M., Pesquer L. G., "Design of an Adaptive Fuzzy Control System for Dual Star Induction Motor Drives," *Advances in Electrical and Computer Engineering,* vol. 18, no. 3, pp. 37-44, 2018.

[13] Boukhalfa G., Belkacem S., Chikhi A., Benaggoune S., "Genetic algorithm and particle swarm optimization tuned fuzzy PID controller on direct torque control of dual star induction motor," *Journal of Central South University,* vol. 26, no. 7, pp. 1886-1896, 2019.

[14] Oumar A., Chakib R., Cherkaoui M., "Performance and Characteristics of Double Star Induction Machine," *8th International Conference on Systems and Control (ICSC),* pp. 1-6, 2019.

[15] Bentouhami L. A., Bendjeddou Y., Merabet E., "Neuro-fuzzy control of a dual star induction machine," *Journal of Power Technologies,* vol. 98, no. 1, pp. 70-79, 2018.

[16] Arbaoui M., Essadki A., Nasser T., Chalawane H., "Comparative Analysis of ADRC & PI Controllers Used in Wind Turbine System Driving a DFIG," *International Journal of Renewable Energy Research*, vol. 7, no. 4, pp. 1816-1824, 2017.

[17] Chakib R., Essadki A., Cherkaoui M., "Modeling and Control of a Wind System based on a DFIG by Active Disturbance Rejection Control," *International Review on Modelling and Simulations,* vol. 7, no. 4, pp. 626-637, 2014.

[18] Wang F., Wang R. J., Liu E., "Analysis and Tuning for Active Disturbance Rejection Control," *Mathematical Problems in Engineering,* vol. 2019, pp. 1-12, 2019.

[19] Chakib M., Nasser T., Essadki A., "Comparative study of active disturbance rejection control with RST control for variable wind speed turbine based on doubly fed induction generator connected to the grid," *International journal of intelligent engineering & systems,* vol. 13, no. 1, pp. 248-258, 2019.

[20] Kuang Z., Du B., Cui S., Chan C. C., "Speed Control of Load Torque Feed Forward Compensation Based on Linear Active Disturbance Rejection for Five-Phase PMSM,*" IEEE Access*, vol. 7, pp. 159787-159796, 2019.

[21] Chakib R., Essadki A., Cherkaoui M., "Participation of DFIG wind turbine controlled by active disturbance rejection control in primary frequency control," *International review of electrical engineering,* vol. 11, no. 12, pp. 183, 2016.

[22] Arbaoui M., Essadki A., Kharchouf I., Nasser T., "A New Robust Control by Active Disturbance Rejection Control Applied on Wind Turbine System Based on Doubly Fed Induction Generator DFIG," *2017 International Renewable and Sustainable Energy Conference (IRSEC),* 2017.

[23] Herbst G., "A Simulative Study on Active Disturbance Rejection Control (ADRC) as a Control Tool for Practitioners," *Electronics,* vol. 2, no. 3, pp. 246-279, 2013.

[24] Rachid Chakib, “Commande avancée d’une éolienne à base de la MADA en vue de sa participation aux services système: réglage de fréquence, réglage de tension et tenue aux creux de tension,” Thesis, Mohammedia School of Engineer, 2017.

[25] Chakib R., Cherkaoui M., Essadki A., “Stator Flux Control by Active Disturbance Rejection Control for DFIG Wind Turbine during Voltage Dip,” *International Journal of Circuits. Systems and Signal Processing,* vol. 9, pp. 281-288, 2015.

[26] Laghridat H., Essadki A., Nasser T., “Comparative Analysis between PI and Linear-ADRC Control of a Grid Connected Variable Speed Wind Energy Conversion System Based on a Squirrel Cage Induction Generator,” *Mathematical Problems in Engineering*, vol. 2019, pp. 1-16, 2019.

[27] Lei Z., Sun X., Xing B., Hu Y., Jin G., “Active disturbance rejection based MPPT control for wind energy conversion system under uncertain wind velocity changes,” *Journal of Renewable and Sustainable Energy*, vol. 10, no. 5, pp. 1-16, 2018.

[28] Hellali L., Belhamdi S., “Speed control of doubly star induction motor (DSIM) using direct field-oriented control (DFOC) based on fuzzy logic controller (FLC),” *Advances in Modelling and analysis C*, vol. 73, no. 4, pp. 128-136, 2018.

BIOGRAPHIES OF AUTHORS

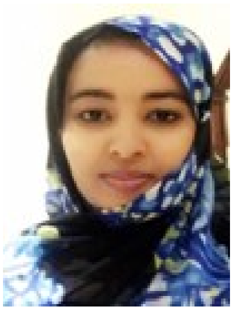

Aichetoune Oumar was born in Akjoujt, Mauritania in 1992. She received the Engineer Degree in Electromechanics Engineering, from Mauritania Mining School (EMIM), Nouakchott, Mauritania, in 2016. She is currently preparing a PhD thesis in the department of Electrical Engineering of Mohammedia School of Engineer (EMI), university Mohamed V, Rabat, Morocco. Her research is about machine control precisely double star induction machine (DSIM).

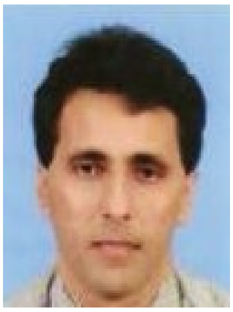

Rachid Chakib was born in Rabat, Morocco in 1973. He received the Engineer Degree in Electrical Engineering, from National Higher School of Electricity and Mechanics (ENSEM), Casablanca, Morocco, in 1997. He received his PhD degree from Mohammedia School of Engineer (EMI), university Mohamed V, Rabat, Morocco in 2017. Prof. CHAKIB is a director of Higher Institut of Engineering and Business (ISGA) Rabat, Morocco.

Mohamed Cherkaoui was born in Marrakech, Morocco in 1954. He received the Engineer Degree in Electrical Engineering, from Mohammedia Engineering School (EMI), Rabat, Morocco, in 1979. He received his PhD degree from Institut National Polytechnique de Lorraine, Nancy, France in 1985. In 1986, he joined the university of Caddi Ayyad of Marrakech as a researcher professor. In 1995, he moves then to the Mohammedia Engineering School (EMI), Rabat, as a professor of higher education and head of Electrical engineering department. Prof. CHERKAOUI is a director of the research laboratory in electrical power and control of the Mohammedia engineering school (EMI), Rabat, Morocco. He is also an expert with Moroccan ministry for higher education and with industrialists to matters related to the energetic efficiency. His main research interests are renewable energy and control of electrical systems.